analytical chemistry

Article

pubs.acs.org/ac

Implementation of Ultraviolet Photodissociation on a Benchtop Q Exactive Mass Spectrometer and Its Application to Phosphoproteomics

Kyle L. Fort,[†,‡] Andrey Dyachenko,[†,‡] Clement M. Potel,[†,‡] Eleonora Corradini,[†,‡] Fabio Marino,[†,‡] Arjan Barendregt,[†,‡] Alexander A. Makarov,[†,§] Richard A. Scheltema,[†,‡] and Albert J. R. Heck*[,†,‡]

[†]Biomolecular Mass Spectrometry and Proteomics, Bijvoet Center for Biomolecular Research and Utrecht Institute of Pharmaceutical Sciences, Utrecht University, 3584 Utrecht, The Netherlands

[‡]Netherlands Proteomics Center, 3584 Utrecht, The Netherlands

[§]Thermo Fisher Scientific (Bremen), 28199 Bremen, Germany

Supporting Information

ABSTRACT: Proteomics applications performed on the popular benchtop Q Exactive Orbitrap mass spectrometer have so far relied exclusively on higher collision-energy dissociation (HCD) fragmentation for peptide sequencing. While this fragmentation technique is applicable to a wide range of biological questions, it also has limitations, and all questions cannot be addressed equally well. Here, we demonstrate that the fragmentation capabilities of the Q Exactive mass spectrometer can be extended with ultraviolet photodissociation (UVPD) fragmentation, complete with synchronization triggering to make it compatible with liquid chromatography (LC)/tandem mass spectrometry (MS/MS) workflows. We show that UVPD not only is directly compatible with LC/MS workflows but also, when combined with these workflows, can result in higher database scores and increased identification rates for complex samples as compared to HCD methods. UVPD as a fragmentation technique offers prompt, high-energy fragmentation, which can potentially lead to improved analyses of labile post-translational modifications. Techniques like HCD result in substantial amounts of modification losses, competing with fragmentation pathways that provide information-rich ion fragments. We investigate here the utility of UVPD for identification of phosphorylated peptides and find that UVPD fragmentation reduces the extent of labile modification loss by up to ~60%. Collectively, when integrated into a complete workflow on the Q Exactive Orbitrap, UVPD provides distinct advantages to the analysis of post-translational modifications and is a powerful and complementary addition to the proteomic toolbox.

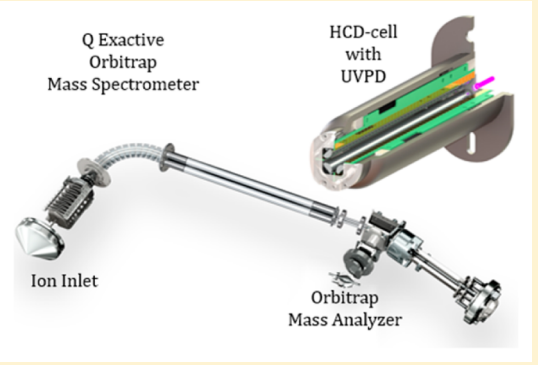

The field of proteomics aims to detect and characterize proteins present in biological samples.[1] With the advent of shotgun proteomics, where proteins are digested into peptides prior to tandem mass spectrometric (MS^2 or MS/MS) analysis, the field has grown immensely in scope and capabilities.[2−4] Even though the complexity of the sample increases manifold, the common properties of peptides ensure that mass spectrometric analysis can largely be performed with a single set of settings. To identify the peptides during postacquisition data analysis, two pieces of information are essential. The first is the precise mass value of the peptides, which in the case of modern mass spectrometry platforms has reached sub-parts per million (ppm) levels and is provided by so-called full or survey scans.[5] The second is supplied by MS^2 or fragmentation scans and consists of the result of mass selection and fragmentation of individual peptide ions, giving rise to ions indicative of the amino acid sequence. To gain speed, fragmentation scans are generally collected at lower mass resolution than full scans. This leads to lower mass precision; however, owing to mass selection in the quadrupole, the mass spectrometer is focused just on the selected peptide ion. An area where shotgun proteomics has significantly contributed is that of post-translational modification (PTM) analysis.[6−9] In a typical shotgun proteomics pipeline, PTMs are retained at the peptide level and can be identified on the basis of the distinct mass difference the modification introduces at both the peptide and fragment-ion levels. However, the choice of fragmentation method has a major impact on how well a particular type of modification can be processed.

Typically, collision-induced dissociation (CID) is utilized to fragment peptides. Here trapped ions are excited by a defined excitation field and subsequently undergo numerous collisions with neutral gas molecules. These collisions slowly transfer energy into the vibrational modes of the ions, ultimately leading

Received: November 3, 2015
Accepted: January 13, 2016
Published: January 13, 2016

DOI: 10.1021/acs.analchem.5b04162
Anal. Chem. 2016, 88, 2303−2310

to fragmentation. The most prominent fragment ions observed with CID peptide fragmentation correspond to low-energy dissociation pathways, such as b- and y-ion formation, owing to this slow heating mechanism. While this provides an excellent dissociation technique for unmodified peptides, the bond between a protein modification and its associated amino acid can be highly labile, causing the fragmentation mass spectrum to be dominated by neutral losses. These neutral losses compete with information-rich fragment ions, limiting the number of informative ions observed. Similar to CID, higher collision-energy dissociation (HCD) accelerates an ion into a neutral gas, causing the formation of low-energy fragment ion types.[10] With HCD, b- and y-ions still undergo neutral loss, albeit less extensively, obstructing identification and site localization. To diminish the extent of neutral losses, the rate of activation and the internal energy obtained by the ion prior to fragmentation need to be increased to access higher-energy fragmentation channels that better preserve labile modifications. Electron capture dissociation (ECD) and electron transfer dissociation (ETD) both provide methods for more prompt fragmentation and have been shown to better preserve modification sites; however, these techniques suffer to a certain degree from low fragmentation efficiencies and require longer (millisecond) reaction times to obtain information-rich fragmentation mass spectra.[11−15] Furthermore, similar to HCD, the ECD and ETD methods have been shown to have charge-state-dependent fragmentation efficiencies.[16−20]

A relative newcomer is ultraviolet photodissociation (UVPD, λ = 193 nm), which utilizes the natural absorbing chromophores present in the backbone of proteins and peptides as well as aromatic amino acids to absorb a high-energy photon emitted through nanosecond-scale laser pulses.[21−26] It has been demonstrated that UVPD causes prompt (less than microsecond) peptide fragmentation and is able to access high-energy fragmentation pathways, such as the formation of a-, c-, x-, and z-ions.[22,27] Owing to the prompt activation, the loss of labile modifications may be expected to be reduced. Collectively, we hypothesized that the prompt activation and production of high-energy fragment ions could make UVPD advantageous for labile PTM analysis on a shotgun proteomics timescale.

One of the most comprehensively studied PTMs is protein phosphorylation of serine, threonine, and tyrosine (STY). This PTM is critical to a large number of biological processes, including cell signaling, biological activity, modification of protein conformation, protein−protein interactions, and modulation of protein function.[28−31] Its biological importance has driven current research efforts in the field of phosphoproteomics, which we extend by integrating UVPD fragmentation into the popular benchtop Q Exactive Orbitrap,[32,33] and we determine the effect of various alterations to instrument performance with a complex cell lysate. To determine the analytical utility of UVPD to phosphoproteomic analysis, our setup was also applied to a standard set of phosphorylated peptides.[34] Analysis of the resulting fragmentation spectra shows that UVPD provides more information-rich spectra than HCD, substantially reduces nonspecific labile modification losses, and can be used for in-depth analysis of phosphoproteomic samples at a nano-liquid chromatography (LC) timescale.

INSTRUMENTATION AND METHODS

Instrumentation Modifications. UVPD was implemented on a Q Exactive Orbitrap mass spectrometer (Thermo Fisher Scientific, Bremen, Germany) through the incorporation of an ExciStar 500 UV laser (Coherent, Santa Clara, CA). To facilitate UVPD capabilities, modification of the HCD-cell was required. These modifications include removal of the charge detector to allow for introduction of the laser beam through a quartz window in a conflat flange and into the HCD-cell. This does not affect the HCD entrance, quadrupole rods, DC gradient lens, or HCD exit lens; thus attenuation of ion transmission by this modification should be minimized (see Figure 1). Upon irradiation, ions are ejected from the HCD-cell

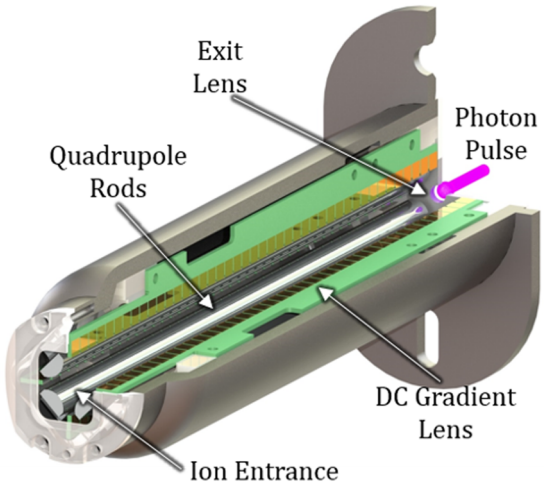

Figure 1. HCD-cell with UVPD capabilities.

for mass analysis. Because no modifications are done to the remainder of the instrument, mass analysis and isolation are not affected by these instrument modifications. For in-depth discussion of the effect of these modifications to the HCD-cell on instrument performance, see Supporting Information (section Effect of IonGun Mode Triggering and Removal of the Charge Detector).

The laser utilizes ArF gas to generate 193 nm photons and generates 6 ns pulses at a repetition rate of up to 500 Hz. Photon pulses, reduced to a diameter of 1.5 mm by use of an optical aperture, are directed into the instrument by high-energy excimer laser mirrors (Edmund Optics, York, U.K.) mounted on micropositioners. Photons are then introduced to the HCD-cell coaxially to the ion packet in order to ensure overlap (see Figure 1). Moreover, this coaxial introduction prevents photons from impacting the ion lenses, minimizing potential effects on ion transmission. We observed that the UV photons do likely hit the C-trap assembly and subsequently produce a set of low-abundance photon-induced ions, detectable in recorded mass spectra. The post-data-acquisition filtering of these background ions is described in Supporting Information under Data Analysis. During typical UVPD operation, the laser energy is maintained at 3 or 5 mJ·pulse^{-1}. The frequency of photon emission is modulated with a delay generator developed in-house, which is synchronized with scan events as described in Supporting Information (section Generation of an External Trigger). All UVPD spectra were generated with 1 laser pulse/scan unless otherwise noted.

DOI: 10.1021/acs.analchem.5b04162
Anal. Chem. 2016, 88, 2303−2310

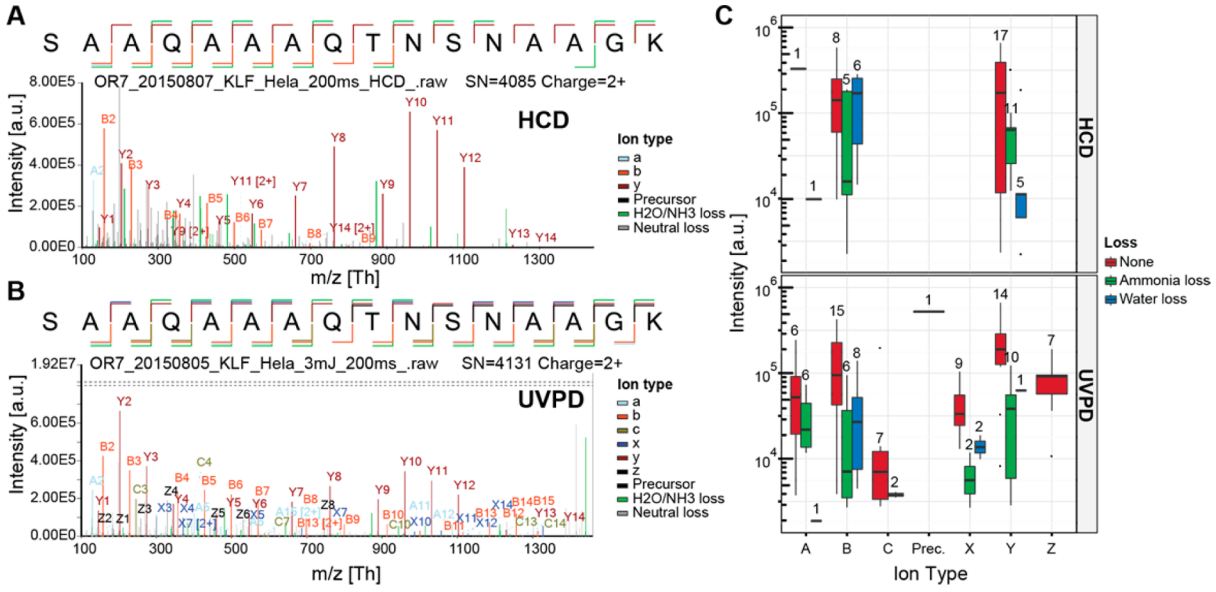

Figure 2. Exemplary spectra obtained with HCD and UVPD fragmentation on the peptide SAAQAAAQTNSNAAGK at high ion injection times. (A) HCD spectrum with fragment ions annotated. (B) UVPD spectrum of the same peptide with fragment ions annotated. The intensity scale is truncated to bring the generally lower intensity UVPD specific fragments into view. (C) Breakdown of different ion types and their contribution in intensity to the fragmentation spectra.

LC/MS Sample Preparation and Data Acquisition. HeLa cells were lysed, reduced and alkylated, and digested overnight at 30 °C with trypsin and Lys C. Phosphoenriched HeLa digest samples were generated by use of Ti-IMAC enrichment as previously described.[35] Both the standard digest and phosphoenriched samples were consequently lyophilized and stored at −80 °C. Prior to LC/MS analysis, the HeLa samples were diluted to a concentration of 250 ng·μL^{-1} with 10% formic acid solution. The phosphoenriched samples were diluted to a final volume of 50 μL with 10% formic acid solution.

Chromatography was performed on both the HeLa digest and phosphoenriched samples, individually, with the Thermo Easy nLC ultra-high-pressure HPLC system (Thermo Fisher Scientific) coupled online to the mass spectrometer with a NanoFlex source (Thermo Fisher Scientific). Analytical columns (50 cm long, 75 μm i.d.) were packed in-house with ReproSil-Pur C_{18} AQ 1.9 μm reversed-phase resin (Dr. Maisch GmbH, Ammerbuch-Entringen, Germany) in buffer A (0.5% acetic acid). During online analysis, the analytical column was heated to 45 °C. Between 0.5 and 1 μg of digested protein was injected onto the column for LC/MS/MS analysis. Mobile phases consisted of 0.1% formic acid (solvent A) and 0.1% formic acid in acetonitrile (solvent B). Mobile-phase elution gradients are presented in Table S1. The eluting peptide solution was ionized via an extruded gold-coated capillary emitter, biased at +1.8 kV with respect to the heated ion inlet. Full mass scans were performed at 70 000 mass resolution, while MS^2 mass scans have a mass resolution of 17 500. Data-dependent mass analysis was performed on the top 10 elution ion signals with a charge state of >1 and <6−8. Dynamic exclusion was maintained at 15 s. HCD analysis was performed at a normalized collision energy (NCE) of 25, unless otherwise noted. UVPD fragmentation was performed as described under Instrumentation Modifications. A single microscan was performed and the maximum ion injection time was set to 120 ms, which corresponds to the sensitive HCD fragmentation mode setting for this instrument.[36] This mode reduces the performance of the instrument in HCD mode by ∼10% at our ion load; however, as UVPD requires a slightly higher ion load and to remove any time factor from the comparison, we have opted to use this setting throughout the experiments. Figure S4 offers a graphical depiction of the timescale of analysis for both UVPD and HCD fragmentation methods. The AGC target for the MS^2 scans in all LC/MS experiments was maintained at 1×10^5. For details on postacquisition data processing and database searching, see the Data Analysis section in Supporting Information.

Direct Injection Sample Preparation of Synthetic Phosphopeptide Standards and Data Acquisition. Aqueous stock solutions of the synthetic phosphopeptides were diluted in 0.1% formic acid to a final concentration of 5 μM. Aliquots of each phosphopeptide solution were loaded into a gold-coated borosilicate glass capillary emitter. Ionization was facilitated by biasing the emitter to +1.2−1.4 kV with respect to the heated ion inlet. All mass spectrometric analysis was performed on an EMR Orbitrap mass spectrometer modified as previously described.[37−39] Implementation of UVPD capabilities on this modified mass spectrometer are identical to those described in the Instrumentation Modifications section. Mass spectra were acquired at 140 000 and 17 500 mass resolution settings. Nitrogen was used as the collision gas within the HCD-cell, and the pressure was adjusted to obtain maximum ion transmission. HCD fragmentation was performed at a NCE of 25, and the charge state setting was matched to the targeted precursor charge state. UVPD fragmentation was performed with ion injection laser triggering and a laser energy of 5 mJ·pulse^{-1}.

RESULTS AND DISCUSSION

We hypothesized that prompt, high-energy fragmentation techniques, such as UVPD, could be advantageous for analysis of peptides with highly labile modifications and other properties hard to analyze with standard fragmentation

DOI: 10.1021/acs.analchem.5b04162
Anal. Chem. 2016, 88, 2303−2310

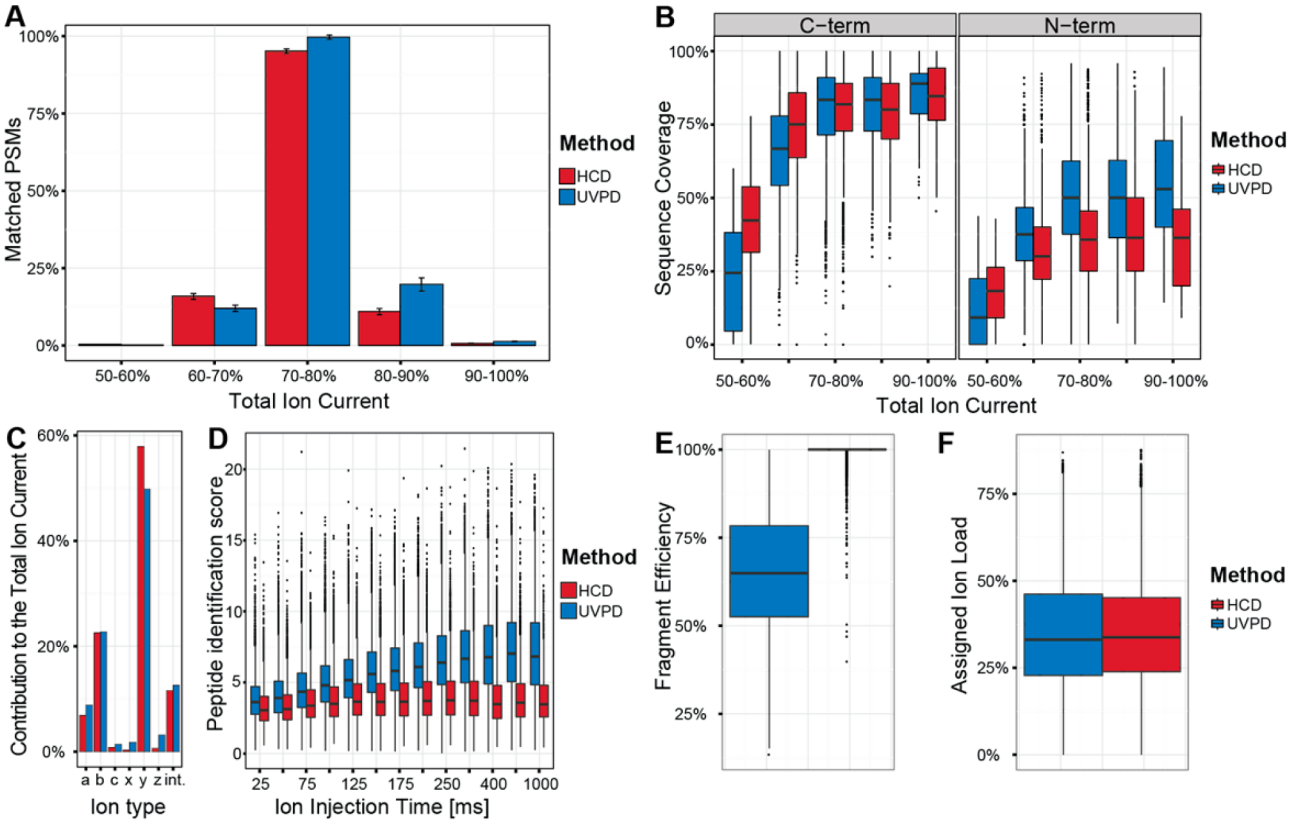

Figure 3. Performance of UVPD vs HCD on a full HeLA digest. (A) Number of matched PSMs of both techniques as a function of the number of ions collected for the fragmentation scan, represented as normalized TIC value in 10% bins. The analysis was performed in triplicate, with the average being displayed and the standard deviation being represented by the error bars. (B) N- and C-terminal fragment coverage as a function of the number of ions collected for the fragmentation scan, represented as normalized TIC value in 10% bins. (C) Contribution of different detected fragment ion types to the TIC of each spectrum between UVPD and HCD. (D) Peptide identification scores as a function of fixed ion injection times, enabling higher ion loads during fragmentation analysis. (E) Fragmentation efficiency comparison of UVPD and HCD. (F) Sum intensity of annotated peaks, excluding precursor-associated fragment peaks.

techniques. However, this demands that modifications to the instrument do not substantially affect its performance in terms of mass analysis or ion transport efficiency. The fragmentation technique must also be able to generate fragmentation mass spectra on a timescale imposed by the online liquid chromatography separation used. Here, the performance of UVPD for analysis of complex proteomes is investigated and described.

Exemplary fragmentation mass spectra of the 16-mer SAAQAAAQTNSNAAGK peptide with HCD (Figure 2A) and UVPD (Figure 2B), collected with the finalized instrument coupled online to liquid chromatography with a maximum ion injection time of 200 ms, illustrate the analytical advantage of UVPD. The HCD spectrum provides 93% sequence coverage and is dominated by a series of b- and y-ions, as well as minor contributions from a-ions (Figure 2C, top). In addition to these standard ion types, the spectrum also contains highly abundant ions corresponding to neutral losses of water and ammonia. UVPD on the same peptide produces a wider range of fragment ion types, a, b, c, x, y, and z, owing to its high-energy fragmentation mechanism and identical sequence coverage of 93% (Figure 2C, bottom). Interestingly, UVPD displays reduced production of fragmentation ions that correspond to neutral losses of water and ammonia, an observation further investigated in the section Proteome-wide UVPD LC/MS. While both fragmentation techniques produce identical sequence coverage, UVPD provides 93% sequence coverage with both N- and C-terminal ions, while HCD shows only 60% sequence coverage with N-terminal ions. This demonstrates that UVPD may give rise to higher sequence coverage, and thus higher confidence in sequence assignment, for ions that have low HCD fragmentation efficiency. In the following discussion we explore the behavior of UVPD and HCD at a full proteome level by investigating the number of peptide spectrum matches (PSMs) achieved by each method. This number is always represented normalized to the maximum number of PSMs in the experiment.

Optimization of UV Photodissociation Settings. Retention of labile modifications critically hinges on minimization of the internal energy in the generated ions during transport, which is deposited by the electric field used to inject the ions into the HCD-cell. To reduce the internal energy and retain the labile modification, the ion injection energy, as modulated by "HCD direct eV setting" within the instrument control software and shown by the NCE filter header, must be as low as possible. If the potential energy drop is too low, however, ion transport efficiency will be negatively affected. Comparison between irradiation with the laser (Figure S1B, blue) and no irradiation (Figure S1B, red) at the lowest HCD ion injection energy shows that UVPD generates identifiable fragment ions. When the laser irradiation is on, a significant increase of ~15% in number of PSMs can be observed between 1 and 2 eV. It can be excluded that these additional PSMs are generated by supplemental collisional activation at the higher

DOI: 10.1021/acs.analchem.5b04162
Anal. Chem. 2016, 88, 2303−2310

energy of 2 eV, as the number of matched PSMs for the control remains <1% at 2 eV. The increase in PSMs observed with laser irradiation is consistent with high transport efficiency, that is, higher total ion current (TIC), at an energy of 2 eV (Figure S1C). At higher levels the extent of collisional dissociation becomes increasingly prominent, as shown by an exponential increase in the number of PSMs at values greater than 5. Such a feature can in the future be utilized to achieve a hybrid combination of UVPD and HCD fragmentation.

The peptide identification score will be used in the next sections as a proxy for the information richness of a fragmentation spectrum.[40] To illustrate, across our series of 10 experiments described above, associated scores for a set of 42 peptides that are consistently identified in each experiment show an increasing trend for peptide identification scores (Figure S1D).

Proteome-wide UV Photodissociation Liquid Chromatography/Mass Spectrometry. Direct comparison of the PSM performance of UVPD to HCD fragmentation on a full HeLa proteome digest as a function of TIC shows that UVPD in our modified setup produces comparable numbers of PSMs as HCD. Breaking up the spectra, based on their TIC normalized to the highest detected TIC value and separated in 10% bins, shows for higher abundant peptide spectra that UVPD produces a slightly higher (∼5−10%) number of PSMs (Figure 3A). Given that the acquisition settings were not altered from a standard LC/MS work flow, that is, one microscan/mass spectrum with a maximum ion injection time of 120 ms, these data show that the timescale for production of UVPD tandem mass spectra is directly compatible with the required timescale for standard proteomic LC/MS analysis. As discussed previously, UVPD produces a wider range of ion types and offers enhanced sequence coverage with N-terminal fragment ions. For MS^2 spectra in the upper 40% of TIC values, that is, TIC of 10^7−10^8, UVPD offers substantially enhanced sequence coverage from N-terminal fragment ions (Figure 3B). Further analysis of the contribution of generated ion types in terms of abundance shows that UVPD produces more c-, x-, and z-ions and slightly reduces the amount of b- and y-ions as compared to HCD (Figure 3C).

Direct comparison of UVPD and HCD over a range of fixed ion injection times (Figure 3D), which limits the introduction of ions into the C-trap by the set time, however, shows that UVPD offers benefit for peptide identification scores with high load samples (>∼10^7) even at the lowest ion injection time of 25 ms (∼5× lower than that used above). The peptide identification score benefit further increases with higher ion injection times for UVPD, indicating that more informative fragment ions keep becoming available for detection with increasing ion loads. For low-load samples, however, such as pulldowns or phosphoenriched samples, this trend demonstrates a clear need for higher-efficiency ionization schemes to be introduced to make full use of the analytical benefit introduced by UVPD.[39] In terms of fragmentation efficiency, UVPD has previously been reported to have low efficiency in depleting the precursor.[22] In our data set we find that UVPD achieves roughly 60% efficiency, while HCD performs in most cases close to 100% when we compare intensity of the remaining precursor to summed intensity of the annotated fragment peaks (Figure 3E). This could potentially lead to difficulties in assigning the peptide sequence when fragment peaks fall out of range. This does not appear to be the case for our data when we compare summed intensity of the annotated peaks to TIC (excluding the precursor for UVPD). Both UVPD and HCD achieve roughly 30% (Figure 3F), where UVPD accesses many more fragmentation pathways, increasing the likelihood of success.

Subproteome UV Photodissociation Liquid Chromatography/Mass Spectrometry. *Low-Load Phosphopeptide Pulldown.* To investigate the performance of UVPD on peptide ions with labile modifications, we compare UVPD to HCD on a phosphorylation-enriched peptide digest. UVPD performed at 3 mJ laser energy generates 30% fewer PSMs than HCD over the full dynamic range of identified peptides (Figure 4A). In an effort to increase the fragmentation efficiency and generate more PSMs, the laser energy was increased to 5 mJ. This results in an increase in the number of generated PSMs; however, even at 5 mJ, UVPD still produces 20% fewer PSMs than HCD. A comparison of the common phosphopeptides matched between the two methods (Figure S5) shows that, with an increase of laser energy, the number of common phosphopeptides matched increases and indicates the improvement is gained with the matching of low-abundance or poorly fragmenting peptides. However, unlike the HeLa digest, we do not gain a significant boost in N-terminal fragment ion sequence coverage (Figure 4B). Like the HeLa digest, UVPD with both energies does gain mostly c-, x-, and z-ions (Figure 4C).

Assignment of fragment ions resulting from neutral losses and loss of the modification itself allows for mapping of the benefit of UVPD over HCD as a fragmentation method for labile modifications. We perform this analysis here by looking for this loss for b- and y- fragment ions in HCD spectra and for all fragment ion types in UVPD spectra. The ratio between modified and unmodified fragment ions is then indicative of the extent of modification loss induced by the respective fragmentation method. For the complete set of phosphopeptides detected in our digest, we find that HCD introduces 15% of this loss, while UVPD introduces 8% (Figure 4D). This marked reduction of 45% helps to direct more ions into the normal fragmentation pathways, providing UVPD with higher specificity when sufficient amounts of ions can be introduced. Comparison to the HeLa data shows for our samples a 10-fold reduction in the ion current at a maximum of 250 ms (Figure 4E).

Direct Infusion of Synthetic Phosphopeptides. To further characterize the performance of UVPD on phosphorylated peptides present at high ion loads we performed experiments with direct infusion, allowing for the introduction of a larger amount of material. This setup was used to analyze a total of 23 uniquely phosphorylated peptides with 1−4 phosphorylations, for which data were collected at different laser energies (3−8 mJ) in continuous and ion injection laser triggering methods (see Supporting Information, section Generation of an External Laser Trigger). These peptides have previously been well-characterized, for instance, also in a direct comparison between HCD and electron transfer and higher-energy collision dissociation (EThcD), and the sequence, analyzable charge states, and modification sites for all peptides investigated are well-known and are listed in Table S2.[34]

HCD displays a series of y-ions accompanied by the neutral loss of H_3PO_4, which have been shown to dominate the mass spectra acquired with CID/HCD fragmentation (Figure 5A).[41] In contrast, the UVPD spectrum collected at 5 mJ laser energy contains only minor phosphate-related modification losses (Figure 5B). Quantified as described previously, UVPD results in 18% modification loss while HCD results in 31%

DOI: 10.1021/acs.analchem.5b04162
Anal. Chem. 2016, 88, 2303−2310

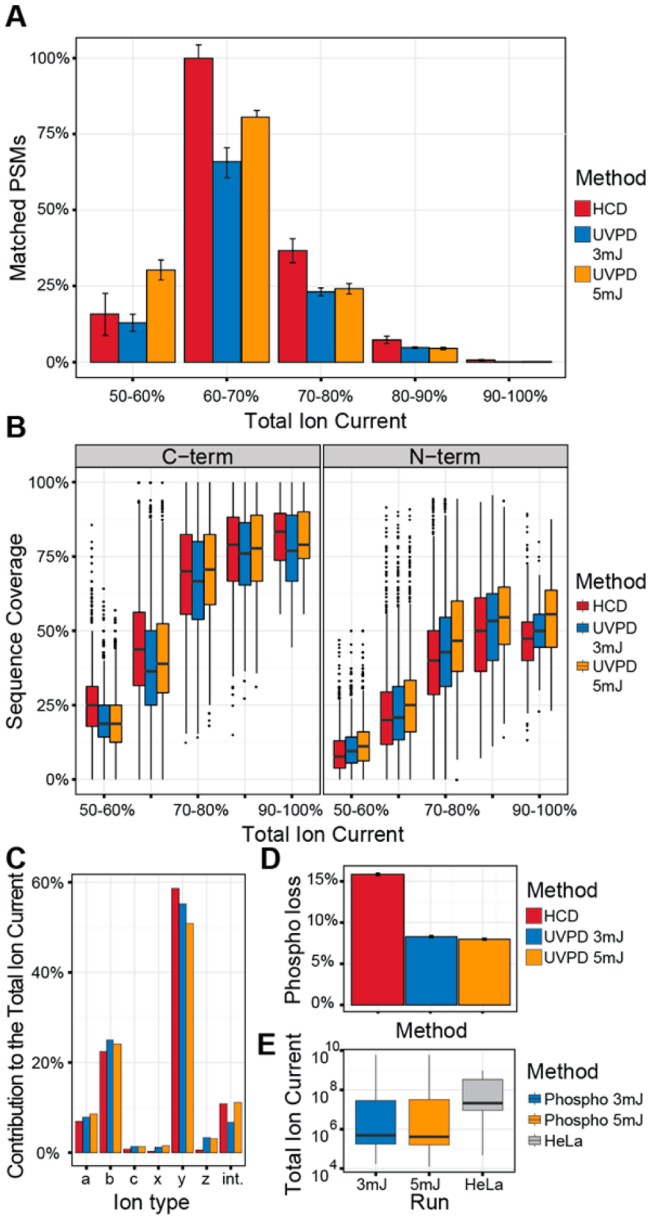

Figure 4. Performance of UVPD versus HCD on a phosphoenriched HeLa digest. (A) Number of matched PSMs of both techniques as a function of number of ions collected for the fragmentation scan. Error bars represent 1 standard deviation of the triplicate experiments. (B) N- and C-terminal fragment coverage as a function of number of ions collected for the fragmentation scan. (C) Contribution of different detected fragment ion types to TIC of each spectrum between UVPD and HCD (int denotes internal fragments). (D) Phosphorylation-group-associated neutral losses expressed as a percentage of total ion current. (E) Total ion current values of phosphorylation samples compared to HeLa digest collected at 250 ms maximum ion injection time.

modification loss. Global analysis of all the peptides reconfirms that UVPD, when compared to HCD, produces significantly less modification loss as shown by reductions of 47%, 40%, 50%, and 58% for singly, doubly, triply, and quadruply phosphorylated peptide ions, respectively (Figure 5C). This higher retention of the modification is directly related to the larger amount of a-, c-, x-, and z-ions, as these ions are high-energy fragment ions produced before energy redistribution within the ion, and small reductions in b- and y-ions, produced by UVPD as compared to HCD (Figure 5D). UVPD still mostly produces b- and y- fragment ions, providing more evidence that supplemental activation is still occurring. This supplemental activation is potentially introduced during transport from the HCD-cell to the Orbitrap analyzer for detection, which can take up to several milliseconds.[42] When only b- and y-ion types are considered, UVPD produces comparable ion scores to HCD; however, upon searching for all ion types, UVPD shows significant increases in ion scores as compared to HCD (Figure 5E).

Comparison between different laser settings shows that, at the lowest energy setting of 3 mJ·pulse^{-1}, modification loss for all peptides investigated could be minimized as compared to all other laser energies investigated (Figure 5F). Upon increasing the laser energy to 8 mJ·pulse^{-1}, modification loss was found to be increased to a maximum value of ∼40%. The increase in modification loss with increased laser energy suggests that extra ion activation is likely occurring as the laser energy is increased from 3 to 8 mJ·pulse^{-1}. As the laser energy is independent of the photon energy and is directly related to the photons per pulse, this suggests that, for peptide ions absorbing more than one photon during analysis, increased activation is introduced. Consistent with this, during continuous irradiation (Figure 5G), where photon emission is no longer correlated to ion injection times and thus multiple irradiation events may occur more frequently, at the highest frequency investigated, modification loss increased to a maximum of ∼47%.

CONCLUSIONS

Work presented here describes modification of the benchtop Q-Exactive Orbitrap mass spectrometer, a popular platform for proteomics applications, to allow for peptide fragmentation by UVPD. As UVPD requires both spatial and temporal synchronization between the photon beam and ion packet, several modifications to our Q Exactive Orbitrap mass spectrometer were required. Systematic investigations revealed that these modifications do not negatively impact the performance of the instrument. Optimizations were made to develop UVPD LC/MS which maximizes proteomic benefits while minimizing the impact of collision-based fragmentation pathways. Benchmark studies of UVPD LC/MS show that UVPD is capable of generating numbers of PSMs comparable to HCD fragmentation methods for analysis of a tryptic HeLa digest. Moreover, owing to the generation of additional high-energy ion types such as a/x and c/z with UVPD methods, the resulting peptide identification scores are also higher than those obtained with HCD fragmentation methods.

Initial UVPD LC/MS analyses of phosphoenriched HeLa digests show that UVPD LC/MS generates significantly fewer fragment ions corresponding to neutral modification loss than HCD LC/MS methods. However, owing to limited ion loads, the benefit of UVPD for these analyses was not fully realized. At higher ion loads, UVPD analysis of a library of synthetic phosphopeptides produces up to 58% less neutral modification loss than HCD. Furthermore, peptide identification of these tandem mass spectra displayed significantly higher identification scores than HCD. It is of interest to consider the similarities between the advantages offered by UVPD and those offered by EThcD for analysis of phosphorylation-enriched samples. Both fragmentation methods generate high-energy ion types and minimize loss of the modification site. As previously shown, EThcD is beneficial to site localization and modification assignment, as well as showing enhanced database scoring.

DOI: 10.1021/acs.analchem.5b04162
Anal. Chem. 2016, 88, 2303−2310

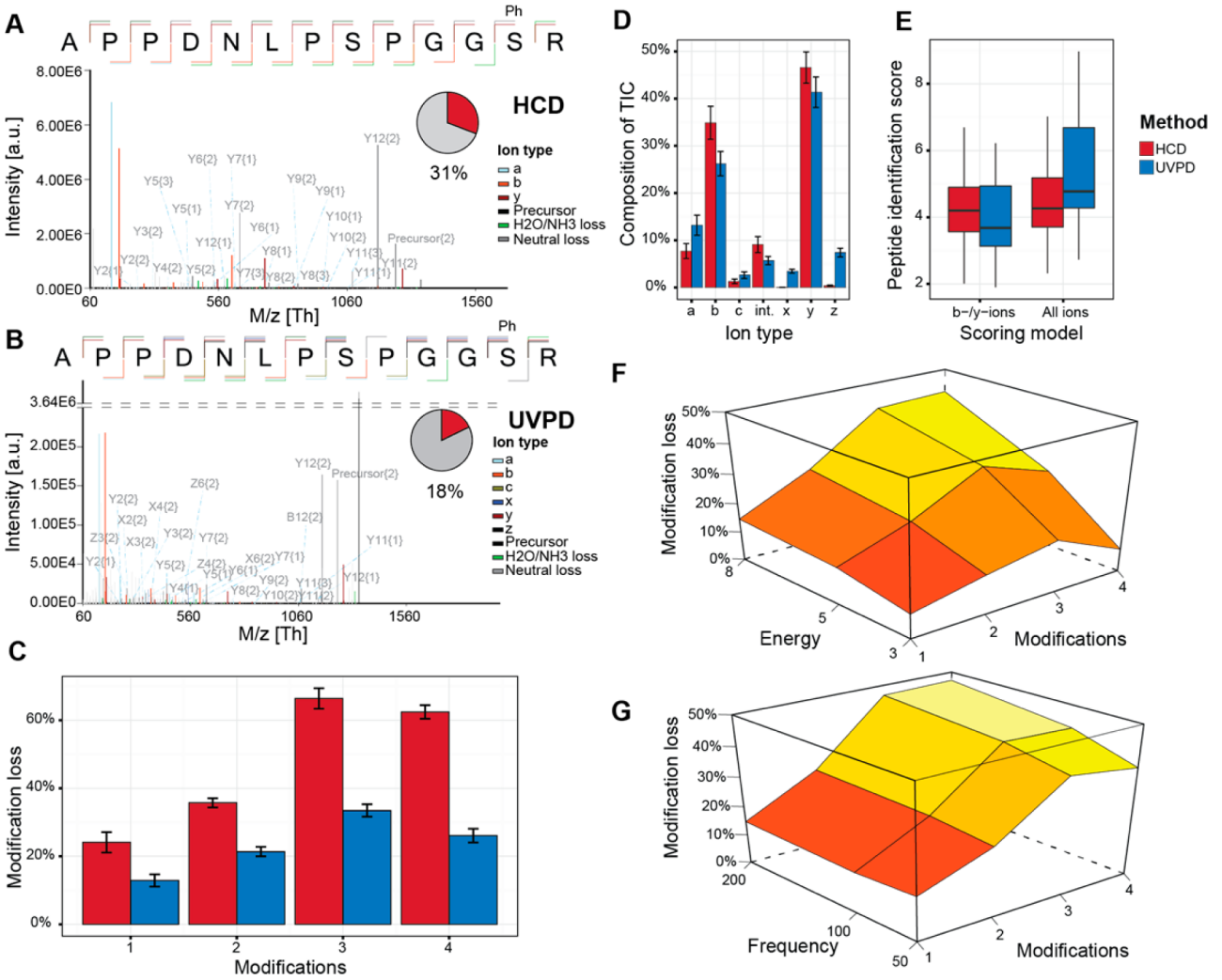

Figure 5. Direct infusion of synthesized phosphopeptides. (A, B) Direct comparison of (A) HCD- and (B) UVPD-generated fragmentation spectra. The modification losses are encoded as {1} $H_3PO_4 + H_2O$, {2} H_3PO_4, and {3} full modification or HPO_3. (Insets) Contribution of neutral losses to TIC. (C) Level of phosphorylation-group-associated neutral losses introduced by both methods, expressed as a percentage of TIC. (D) Contribution of different ion types, expressed as a percentage of TIC (int denotes internal fragments). Error bars represent 1 standard deviation. (E) Peptide identification scores for HCD and UVPD, obtained by searching only for b- and y-ions and enabling all ions. (F) Contribution of neutral losses to TIC as a function of laser energy and number of modifications. (G) Contribution of neutral losses to TIC as a function of laser pulse frequency and number of modifications.

Here, UVPD produces similar enhancements and advantages to traditional methods.

Currently, when utilized in LC/MS workflows with high peptide loads, UVPD is performing comparably to HCD, a technique that has been fully optimized in terms of instrumentation and data analysis. This shows the great promise of UVPD and suggests, on the basis of our results with fixed ion injection times plateauing at 200 ms (Figure 3D), that with a moderate 2−4× boost in ion loads the full potential of UVPD can be realized. Such a boost enables the detection of currently low-abundance fragment ions and is within reach with ongoing developments in ionization efficiency[39] and chromatography.[43,44] Moreover, our data represent a first indication of the advantage of UVPD for analysis of phosphate moieties on peptides at a proteome-wide and LC/MS-compatible scale. With this, we foresee that UVPD will become a valuable addition to the proteomics toolbox.

■ ASSOCIATED CONTENT

Supporting Information

The Supporting Information is available free of charge on the ACS Publications website at DOI: 10.1021/acs.analchem.5b04162.

Additional text sections describing effect of IonGun mode triggering and removal of charge detector, generation of an external laser trigger, data analysis, and production of specific fragment ions; six figures showing instrument performance, database scores for HeLa digest before and after modification, representation of electrical potentials used within HCD and UVPD mode of operation, graphical depiction of the timescale of ion transport, activation, and mass analysis, comparison of identified phophopeptide ions, and presence of UPVD-specific fragments where higher counts for a fragmentation method implies that this particular ion is more frequent for that method; three tables listing LC

DOI: 10.1021/acs.analchem.5b04162
Anal. Chem. 2016, 88, 2303−2310

gradients for various samples, phosphopeptide library, and raw files correlated to figures (PDF)

AUTHOR INFORMATION

Corresponding Author

*Phone +31-030-253-6797; e-mail a.j.r.heck@uu.nl.

Notes

The authors declare no competing financial interest.

ACKNOWLEDGMENTS

We thank the group of Jennifer Brodbelt (University of Texas, Austin) for advice in implementing the UV laser in our setup. We thank Karl Mechtler (IMP, Vienna, Austria) for providing the synthetic phosphopeptide standard. We thank Maarten Altelaar, Simone Lemeer, and Celine Mulder for discussions and providing HeLa phosphorylation extracts. We thank Martin Fitzpatrick for discussions and his programming expertise. Part of this research was performed within the framework of the PRIME-XS project, Grant 262067, funded by the European Union Seventh Framework Program, and The Netherlands Organization for Scientific Research (NWO) supported large-scale proteomics facility Proteins@Work (Project 184.032.201) embedded in The Netherlands Proteomics Centre. A.A.M. and A.J.R.H. acknowledge additional support through the European Union Horizon 2020 programme FET-OPEN project MSmed, Project 686547.

REFERENCES

(1) Aebersold, R.; Mann, M. *Nature* **2003**, *422*, 198−207.
(2) Altelaar, A. F. M.; Munoz, J.; Heck, A. J. R. *Nat. Rev. Genet.* **2013**, *14*, 35−48.
(3) Bensimon, A.; Heck, A. J. R.; Aebersold, R. *Annu. Rev. Biochem.* **2012**, *81*, 379−405.
(4) Zhang, Y. Y.; Fonslow, B. R.; Shan, B.; Baek, M. C.; Yates, J. R. *Chem. Rev.* **2013**, *113*, 2343−2394.
(5) Olsen, J. V.; de Godoy, L. M. F.; Li, G.; Macek, B.; Mortensen, P.; Pesch, R.; Makarov, A.; Lange, O.; Horning, S.; Mann, M. *Mol. Cell. Proteomics* **2005**, *4*, 2010−2021.
(6) Engholm-Keller, K.; Larsen, M. R. *Proteomics* **2013**, *13*, 910−931.
(7) Zhao, Y. M.; Jensen, O. N. *Proteomics* **2009**, *9*, 4632−4641.
(8) Grimsrud, P. A.; Swaney, D. L.; Wenger, C. D.; Beauchene, N. A.; Coon, J. J. *ACS Chem. Biol.* **2010**, *5*, 105−119.
(9) Olsen, J. V.; Blagoev, B.; Gnad, F.; Macek, B.; Kumar, C.; Mortensen, P.; Mann, M. *Cell* **2006**, *127*, 635−648.
(10) Nagaraj, N.; D'Souza, R. C. J.; Cox, J.; Olsen, J. V.; Mann, M. *J. Proteome Res.* **2012**, *11*, 3506−3508.
(11) Shi, S. D. H.; Hemling, M. E.; Carr, S. A.; Horn, D. M.; Lindh, I.; McLafferty, F. W. *Anal. Chem.* **2001**, *73*, 19−22.
(12) Sweet, S. M. M.; Bailey, C. M.; Cunningham, D. L.; Heath, J. K.; Cooper, H. J. *Mol. Cell. Proteomics* **2009**, *8*, 904−912.
(13) Kelleher, N. L.; Zubarev, R. A.; Bush, K.; Furie, B.; Furie, B. C.; McLafferty, F. W.; Walsh, C. T. *Anal. Chem.* **1999**, *71*, 4250−4253.
(14) Wiesner, J.; Premsler, T.; Sickmann, A. *Proteomics* **2008**, *8*, 4466−4483.
(15) Compton, P. D.; Strukl, J. V.; Bai, D. L.; Shabanowitz, J.; Hunt, D. F. *Anal. Chem.* **2012**, *84*, 1781−1785.
(16) Zubarev, R. A.; Horn, D. M.; Fridriksson, E. K.; Kelleher, N. L.; Kruger, N. A.; Lewis, M. A.; Carpenter, B. K.; McLafferty, F. W. *Anal. Chem.* **2000**, *72*, 563−573.
(17) Olsen, J. V.; Haselmann, K. F.; Nielsen, M. L.; Budnik, B. A.; Nielsen, P. E.; Zubarev, R. A. *Rapid Commun. Mass Spectrom.* **2001**, *15*, 969−974.
(18) Iavarone, A. T.; Paech, K.; Williams, E. R. *Anal. Chem.* **2004**, *76*, 2231−2238.
(19) Good, D. M.; Wirtala, M.; McAlister, G. C.; Coon, J. J. *Mol. Cell. Proteomics* **2007**, *6*, 1942−1951.
(20) Frese, C. K.; Altelaar, A. F. M.; Hennrich, M. L.; Nolting, D.; Zeller, M.; Griep-Raming, J.; Heck, A. J. R.; Mohammed, S. *J. Proteome Res.* **2011**, *10*, 2377−2388.
(21) Reilly, J. P. *Mass Spectrom. Rev.* **2009**, *28*, 425−447.
(22) Brodbelt, J. S. *Chem. Soc. Rev.* **2014**, *43*, 2757−2783.
(23) Madsen, J. A.; Kaoud, T. S.; Dalby, K. N.; Brodbelt, J. S. *Proteomics* **2011**, *11*, 1329−1334.
(24) Ko, B. J.; Brodbelt, J. S. *J. Am. Soc. Mass Spectrom.* **2011**, *22*, 49−56.
(25) Joly, L.; Antoine, R.; Broyer, M.; Dugourd, P.; Lemoine, J. *J. Mass Spectrom.* **2007**, *42*, 818−824.
(26) Halim, M.; Girod, M.; MacAleese, L.; Lemoine, J.; Antoine, R.; Dugourd, P. *J. Am. Soc. Mass Spectrom.* **2015**, DOI: 10.1007/s13361-015-1297-5.
(27) Cammarata, M. B.; Brodbelt, J. S. *Chemical Science* **2015**, *6*, 1324−1333.
(28) Prvulovic, D.; Hampel, H. *Clin. Chem. Lab. Med.* **2011**, *49*, 367.
(29) Davidsson, P.; Sjögren, M. *Dis. Markers* **2005**, *21*, 81−92.
(30) Wang, Z.; Gucek, M.; Hart, G. W. *Proc. Natl. Acad. Sci. U. S. A.* **2008**, *105*, 13793−13798.
(31) Yachie, N.; Saito, R.; Sugiyama, N.; Tomita, M.; Ishihama, Y. *PLoS Comput. Biol.* **2011**, *7*, No. e1001064.
(32) Michalski, A.; Damoc, E.; Hauschild, J. P.; Lange, O.; Wieghaus, A.; Makarov, A.; Nagaraj, N.; Cox, J.; Mann, M.; Horning, S. *Mol. Cell. Proteomics* **2011**, *10*, No. M111.011015.
(33) Scheltema, R. A.; Hauschild, J. P.; Lange, O.; Hornburg, D.; Denisov, E.; Damoc, E.; Kuehn, A.; Makarov, A.; Mann, M. *Mol. Cell. Proteomics* **2014**, *13*, 3698−3708.
(34) Frese, C. K.; Zhou, H.; Taus, T.; Altelaar, A. F. M.; Mechtler, K.; Heck, A. J. R.; Mohammed, S. *J. Proteome Res.* **2013**, *12*, 1520−1525.
(35) Zhou, H.; Ye, M.; Dong, J.; Han, G.; Jiang, X.; Wu, R.; Zou, H. *J. Proteome Res.* **2008**, *7*, 3957−3967.
(36) Kelstrup, C. D.; Young, C.; Lavallee, R.; Nielsen, M. L.; Olsen, J. V. *J. Proteome Res.* **2012**, *11*, 3487−3497.
(37) Snijder, J.; van de Waterbeemd, M.; Damoc, E.; Denisov, E.; Grinfeld, D.; Bennett, A.; Agbandje-McKenna, M.; Makarov, A.; Heck, A. J. R. *J. Am. Chem. Soc.* **2014**, *136*, 7295−7299.
(38) Rose, R. J.; Damoc, E.; Denisov, E.; Makarov, A.; Heck, A. J. R. *Nat. Methods* **2012**, *9*, 1084−1086.
(39) Belov, M. E.; Damoc, E.; Denisov, E.; Compton, P. D.; Horning, S.; Makarov, A. A.; Kelleher, N. L. *Anal. Chem.* **2013**, *85*, 11163−11173.
(40) Eng, J.; McCormack, A.; Yates, J. *J. Am. Soc. Mass Spectrom.* **1994**, *5*, 976−989.
(41) Boersema, P. J.; Mohammed, S.; Heck, A. J. R. *J. Mass Spectrom.* **2009**, *44*, 861−878.
(42) Kim, T. Y.; Reilly, J. P. *J. Am. Soc. Mass Spectrom.* **2009**, *20*, 2334−2341.
(43) Hahne, H.; Pachl, F.; Ruprecht, B.; Maier, S. K.; Klaeger, S.; Helm, D.; Medard, G.; Wilm, M.; Lemeer, S.; Kuster, B. *Nat. Methods* **2013**, *10*, 989.
(44) Zhou, F.; Lu, Y.; Ficarro, S. B.; Webber, J. T.; Marto, J. A. *Anal. Chem.* **2012**, *84*, 5133−5139.

DOI: 10.1021/acs.analchem.5b04162
Anal. Chem. 2016, 88, 2303−2310